K^+ Channels of Stomatal Guard Cells

Characteristics of the Inward Rectifier and Its Control by pH

MICHAEL R. BLATT

From the Botany School, University of Cambridge, Cambridge CB2 3EA, United Kingdom

ABSTRACT Intracellular microelectrode recordings and a two-electrode voltage clamp have been used to characterize the current carried by inward rectifying K^+ channels of stomatal guard cells from the broadbean, *Vicia faba* L. Superficially, the current displayed many features common to inward rectifiers of neuromuscular and egg cell membranes. In millimolar external K^+ concentrations (K_o^+), it activated on hyperpolarization with half-times of 100–200 ms, showed no evidence of time- or voltage-dependent inactivation, and deactivated rapidly ($\tau \sim 10$ ms) on clamping to 0 mV. Steady-state conductance–voltage characteristics indicated an apparent gating charge of 1.3–1.6. Current reversal showed a Nernstian dependence on K_o^+ over the range 3–30 mM, and the inward rectifier was found to be highly selective for K^+ over other monovalent cations ($K^+ > Rb^+ > Cs^+ \gg Na^+$). Unlike the inward rectifiers of animal membranes, the current was blocked by charybdotoxin and α-dendrotoxin ($K_d \ll 50$ nM), as well as by tetraethylammonium chloride ($K_{1/2} = 9.1$ mM); gating of the guard cell K^+ current was fixed to voltages near −120 mV, independent of K_o^+, and the current activated only with supramillimolar K^+ outside ($E_K^+ > -120$ mV). Most striking, however, was inward rectifier sensitivity to $[H^+]$ with the K^+ current activated reversibly by mild acid external pH. Current through the K^+ inward rectifier was found to be largely independent of intracellular pH and the current reversal (equilibrium) potential was unaffected by pH_o from 7.4 to 5.5. By contrast, current through the K^+ outward rectifier previously characterized in these cells (1988. *J. Membr. Biol.* 102:235) was largely insensitive to pH_o, but was blocked reversibly by acid-going intracellular pH. The action of pH_o on the K^+ inward rectifier could not be mimicked by extracellular Ca^{2+} for which changes in activation, deactivation, and conductance were consonant with an effect on surface charge ($[Ca^{2+}] \leq 1$ mM). Rather, extracellular pH affected activation and deactivation kinetics disproportionately, with acid-going pH_o raising the K^+ conductance and shifting the conductance–voltage profile positive-going along the voltage axis and into the physiological voltage range. Voltage and pH dependencies for gating were consistent with a single, titratable group ($pK_a \sim 7$ at −200 mV) residing deep within the membrane electric field and accessible from the outside. The high

Dr. Blatt's present address and address for correspondence is Department of Biochemistry and Biological Sciences, University of London, Wye College, Wye, Kent TN25 5AH, England.

J. GEN. PHYSIOL. © The Rockefeller University Press · 0022-1295/92/04/0615/30 $2.00 615
Volume 99 April 1992 615–644

sensitivity of the K^+ inward rectifier to $[H^+]_o$ presents a mechanistic basis for understanding K^+ channel and H^+-ATPase integration over a wide range of environmental conditions, and the H^+ sensitivities of both K^+ inward and outward rectifiers intimate roles for pH in controlling K^+ flux during stomatal movements.

INTRODUCTION

It is now generally accepted that K^+ channels in the guard cell plasma membrane[1] provide the dominant pathway for K^+ flux, at least during stomatal closing (Blatt, 1991*a*). K^+ channels that rectify strongly outward have been identified both in intact guard cells (Blatt, 1988*a*) and in their protoplasts (Schroeder et al., 1987; Hosoi et al., 1988). In the intact cells, gating of these channels is dependent on K^+ and ensures that an outward bias to K^+ flux is maintained in the face of a variable external K^+ concentration (Blatt, 1988*a*, *b*, 1991*b*). Ensemble channel current is augmented by the phytohormone abscisic acid which promotes stomatal closure (Blatt, 1990; Thiel et al., 1992), and the fungal toxin fusicoccin, which evokes irreversible stomatal opening, inactivates the channels and effectively blocks K^+($^{86}Rb^+$) tracer efflux from guard cells (Blatt and Clint, 1989; Clint and Blatt, 1989).

Until recently, evidence supporting channel activity for K^+ uptake during stomatal opening has been less clear cut. Such a function has been ascribed to a second class of K^+ channels, originally identified through patch electrode studies with guard cell protoplasts (Schroeder et al., 1987), based on the observation that these channels rectify strongly inward. The strongest evidence has come from parallel studies linking changes in channel gating and a depression in current carried by the inward rectifier to abscisic acid and a rise in cytoplasmic free Ca^{2+} concentration (Schroeder and Hagiwara, 1989; Blatt et al., 1990*b*; Gilroy et al., 1990; McAinsh et al., 1990). This response, along with membrane depolarizations, may be seen to prevent K^+ uptake during stomatal closure.

Even so, there are aspects of inward rectifier behavior that appear to conflict with its postulated role in K^+ uptake. Among others, the voltage dependence for current activation has been reported to be insensitive to the external K^+ (K_o^+) environment (Schroeder, 1988), thus raising doubts about its ability to function under K^+-limiting conditions. As Clint and Blatt (1989) point out, situations are easily found—notably at acid pH_o and low K_o^+—in which a channel exhibiting such behavior would mediate K^+ loss from, rather than K^+ uptake into the guard cells. Furthermore, net K^+ uptake has been observed even when the prevailing driving force was for K^+ efflux from the guard cell (Clint and Blatt, 1989).

These studies must raise questions about the multiplicity of inherent controls on channel activity as well as about channel integration with the stomatal environment and parallel transport activities at the guard cell plasma membrane. Indeed, the inward rectifier has been seen only infrequently in guard cell protoplasts (cf. Hosoi et al., 1988) and, even in the intact cells, is evident only after prior exposure to high (≥ 10 mM) K_o^+ (Blatt et al., 1990*b*). Bearing in mind the sensitivity of the K^+ inward

[1] For reasons detailed previously (Blatt et al., 1990*b*), electrical recordings from the guard cells are assumed to reflect the characteristics of the plasma membrane alone. I use the terms guard "cell" and "membrane" potential, current, and conductance in this context.

rectifier to intracellular Ca^{2+}, I began a systematic analysis of conditions that might complement cellular control of pCa_i. A limited response to extracellular Ca^{2+} was observed, consistent with charge screening at the membrane surface and, at high external concentrations, a parallel influence on pCa_i; but the most striking features of the K^+ inward rectifier proved to be its sensitivity to pH, with mild acid conditions activating the current and altering its steady-state conductance–voltage profile. This paper documents the influence of pH, of external Ca^{2+} and K^+ on the K^+ inward rectifier, as well as related characteristics of channel permeation and block. The results indicate that the effects of $[H^+]$ on inward rectifier current are mediated by H^+ from the outside. Current through the K^+ outward rectifier, likewise, is shown to be H^+ sensitive, but, in this case, to $[H^+]$ on the cytoplasmic side of the membrane. Both intracellular and extracellular pH dependencies carry important implications for K^+ channel function and its integration with the primary H^+-ATPase of guard cells in situ. Thus, overall, the data establish a basis for transport control by H^+ allied to, but distinct from, the role of the cation in energization of the plant plasma membrane.

MATERIALS AND METHODS

Plant Culture and Experimental Protocol

The experiments for this study were carried out during the winter months between November and February. *Vicia faba* L., cv. (Bunyan) Bunyard Exhibition, was grown on vermiculite with Hoagland's Salts medium and epidermal strips were prepared as described before from newly expanded leaves taken 4–6 wk after sowing (Blatt, 1987*a*, *b*). Measurements were carried out in rapidly flowing solutions (10 ml/min, ~20 chamber volumes/min). Ambient temperatures were 20–22°C. Standard buffers were prepared with 5 or 10 mM HEPES (pK_a 7.4) or 2-(2-(hydroxy-1,1-bis(hydroxymethyl-)ethyl)amino) ethanesulfonic acid (TES, pK_a 7.4), 2-(*N*-morpholino)propanesulfonic acid (MES, pK_a 6.1), and 2-(hydroxy-1,1-bis(hydroxymethyl)-ethyl)amino-1-propanesulfonic acid (TAPS, pK_a 8.4) at the respective pK_a values. Buffer solutions were titrated with $Ca(OH)_2$ (final $[Ca^{2+}]$ ~1 mM) or, for experiments in which $[Ca^{2+}]_o$ was varied, with NaOH, in which case Ca^{2+} was added as the Cl^- salt. Intermediate pH values were achieved by adjusting the buffer concentration to maintain $[Ca^{2+}]$ constant. In other experiments, the buffers were titrated with NaOH to achieve a range of pH values to which 1 mM $CaCl_2$ was added. Potassium and other salts were included as required. Butyrate (pK_a 4.81) was added after titrating with NaOH to the specified pH.

Surface areas and volumes of impaled cells were calculated assuming a cylindrical geometry (Blatt, 1987*a*). The orthogonal dimensions (diameter, length) of the cells and stomatal apertures were measured with a calibrated eyepiece micrometer. Cell dimensions in these experiments typically varied over 10–14 μm (diameter) and 35–40 μm (length). Estimated surface areas thus were 1.9×10^{-5}–2.8×10^{-5} cm^2 and cell volumes were 2.7–7.1 pl.

Electrical

Mechanical, electrical, and software designs have been described in detail (Blatt, 1987*a*, *b*, 1990, 1991*b*). Epidermal peels fixed to the glass bottom of the experimental chamber after coating the chamber surface with an optically clear and pressure-sensitive silicone adhesive (no. 355 medical adhesive; Dow Corning, Brussels, Belgium), and all operations were carried out on a Zeiss IM inverted microscope (Zeiss, Oberkochen, Germany) fitted with Nomarski Differential Interference Contrast optics.

Recordings were obtained using double-barreled microelectrodes (Blatt, 1987*a*, 1991*b*). The

electrodes were filled with 200 mM K^+-acetate, pH 7.3, to minimize salt leakage and salt-loading artifacts (Blatt, 1987*a*), and were coated with paraffin to reduce electrode capacitance. Connection to the amplifier headstage was via a 1 M KCl/Ag-AgCl half-cell, and a matching half-cell and 1 M KCl-agar bridge served as the reference (bath) electrode.

Current–voltage (*I-V*) relations were determined by the two-electrode method with the voltage clamp under microprocessor control. Steady-state *I–V* relations were recorded by clamping cells to a bipolar staircase of command voltages (Blatt, 1987*b*). Steps alternated positive and negative from the free-running membrane potential, V_m (typically 20 bipolar pulse pairs) and were separated by equivalent periods when the membrane was clamped to V_m. The current signal was filtered by a six-pole Butterworth filter at 1 or 3 kHz (−3 dB) before sampling, and currents and voltages were recorded during the final 10 ms of each pulse.

For time-dependent characteristics, current and voltage were sampled continuously at 1, 2, or 10 kHz while the clamped potential was driven through cycles of one to four programmable pulse steps. In all cases the holding potential was set to V_m at the start of the clamp cycle. Recordings at 10 kHz (above the Nyquist limit) were restricted by available data storage space to 200-ms "windows" within each cycle; otherwise data taken at all frequencies gave similar results. The sampling rate for most of the data shown was 2 kHz. No attempt was made to compensate for the series resistance (R_s) to ground (Hodgkin et al., 1952). Estimates for R_s indicated that it was unlikely to pose a serious problem in measurements of clamp potential (Blatt, 1988*a*), despite the often high resistivity of the bathing media (=2.5 kΩ cm for 5 mM Ca^{2+}-HEPES with 0.1 mM KCl).

Numerical Analysis

Preliminary data analysis was carried out by nonlinear, least-squares methods (Marquardt, 1963) and, where appropriate, results are reported as the mean ± standard error of n observations.

Chemicals and Solutions

Tetraethylammonium chloride and the pH buffers were from Sigma Chemical Co. (St. Louis, MO). Otherwise, all chemicals were analytical grade from BDH Ltd. (Poole, Dorset, UK). Charybdotoxin (from Prof. C. Miller, Brandeis University, Boston, MA) and α-dendrotoxin (from Prof. J. O. Dolly, Imperial College, London, UK) were prepared as aqueous stock solutions and stored at 0–5°C.

RESULTS

Preliminary Observations in High K_o^+ and Acid pH

Previous studies have shown that, after the growing season (September/October and thereafter), guard cells generally exhibit little evidence of primary pump activity, as can be determined from their electrical characteristics (compare Blatt, 1987*a*, *b*; Thiel et al., 1992; and Blatt, 1988*b*; Blatt and Clint, 1989; Blatt, 1990), thus greatly simplifying investigations of the underlying channel activities. Under these conditions, and even on superfusion with 1–10 mM K_o^+, little or no measurable inward current was observed above the background instantaneous or "leak" current. A time-dependent inward current was usually evoked on raising K_o^+ to 30 mM or after prolonged (5–15 min) exposure to 10 mM K_o^+, after which the current was evident also when K_o^+ was reduced to concentrations as low as 1–3 mM. Fig. 1 shows the time-dependent and steady-state characteristics of the current typical of recordings in

30 mM K_o^+ (5 mM Ca^{2+}-HEPES or Ca^{2+}-TES, pH 7.4). The current was characterized by its activation on clamping to voltages negative of approximately −120 mV and by its apparent lack of any time- or voltage-dependent inactivation, even over periods of 10–20 s (not shown). Current activation was roughly exponential in trajectory, although some sigmoidicity was occasionally evident at the more positive voltages. Activation half-times ranged between ~100 and 200 ms; current deactivation approximated a simple exponential decay with time constants $\tau < 60$ ms at voltages near and positive of −100 mV (see also Figs. 3 and 4).

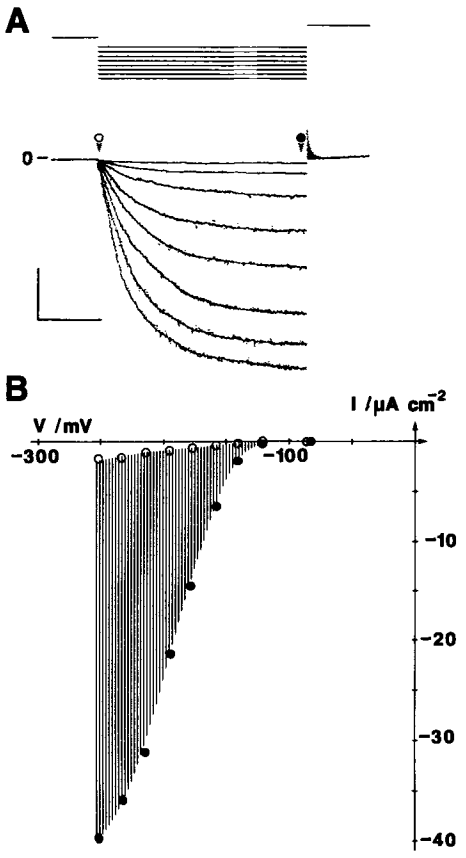

FIGURE 1. Activation, deactivation, and steady-state characteristics of the inward rectifier of a *Vicia* guard cell. Data gathered in 5 mM Ca^{2+}-HEPES, pH 7.4, with 30 mM KCl. (*A*) Time-dependent characteristics. Clamp protocol (eight cycles, above): holding voltage (V_m), −45 mV (not shown); conditioning voltage, −80 mV; test voltages, −120 to −250 mV; tailing voltage, −30 mV. Current records (below) with the zero level indicated on the left. Scale: vertical, 200 mV or 10 μA cm^{-2}; horizontal, 300 ms. (*B*) Instantaneous (○) and steady-state (●) *I-V* curves cross-referenced by symbol to their corresponding time points on the current record in *A*. Note the absence of a time-independent component to the inward rectifier. *Shading*, steady-state K^+ current. Cell parameters: surface area, $1.9 \cdot 10^{-5}$ cm^2; volume, 4.9 pl; stomatal aperture, 7 μm.

Fig. 2 shows the time course with which the inward rectifier developed in the same cell. In this case, steady-state currents were assayed using a bipolar staircase protocol (see Material and Methods) to minimize sampling time without sacrificing the voltage span; *I-V* scans (scan durations, 10–20 s, depending on the number of data points) were run on the same cell before and at intervals after superfusion 10 mM K_o^+. It must be stressed that the evolution of the current is unrelated to the time required for solution exchange in the bath or in the unstirred layer of the cell wall; solution exchanges were complete within 5–10 s ($t_{1/2}$ ~2–3 s), as could be determined from

tip potentials of partially blocked microelectrodes, from the free-running voltage response of the guard cells (see Fig. 2, *insets*) and from shifts in tail current reversal potentials of the outward rectifying K^+ current (not shown). Returning the guard cells to buffer with 0.1 mM K_o^+ eliminated the current but, once evoked, it was always recovered immediately on subsequent transfer to 3–30 mM K_o^+. Nor did the current show any measurable dependence on the choice of anion added with K^+ (Cl^-, SO_4^{2-}, or MES at pH 7.4, data not shown). Furthermore, preliminary experiments revealed that this conditioning period was superfluous when guard cells were impaled in, or transferred to equivalent solutions buffered at acid pH. Lowering the pH of the bath

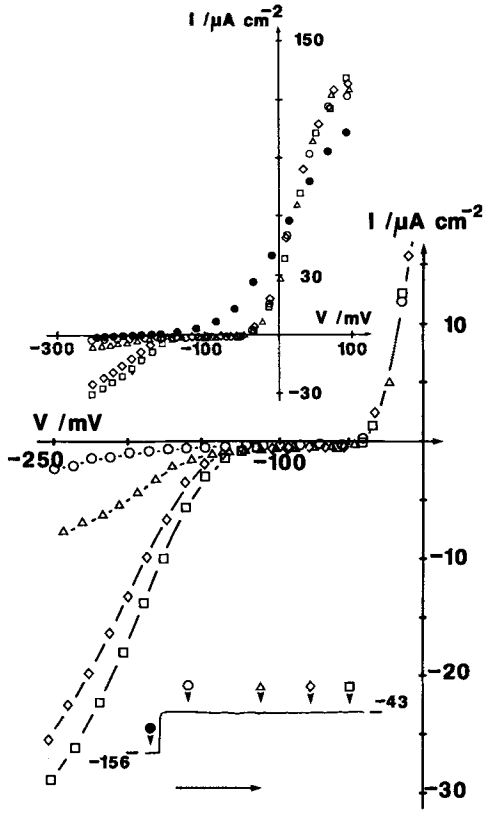

FIGURE 2. Time course for development of the inward rectifier at alkaline pH. Data are from the same guard cell as in Fig. 1. The figure shows the detail of steady-state *I-V* curves gathered using a bipolar staircase protocol (step duration, 700 ms) with the cell bathed in 5 mM Ca^{2+}-HEPES, pH 7.4, with 30 mM KCl. (*Inset above*) Complete *I-V* scans, including data gathered initially in buffer with 0.1 mM KCl (●). (*Inset below*) Voltage trace with *I-V* scans masked from trace. Symbols indicate the times at which the *I-V* scans were taken (cross-referenced by symbol). Exposure to 10 mM K_o^+ marked by depolarization to ~ −40 mV. Contrast the immediate response of the outward rectifier with that of the inward rectifier on transfer to 30 mM K_o^+. After evoking the K^+ inward rectifier, repeated transfers between 0.1 and 30 mM K_o^+ resulted in the loss (0.1 mM) and recovery (30 mM) of the current within the time frame of solution exchange in the chamber (not shown). Current characteristics in 0.1 mM K_o^+ were superimposable with the data shown (●).

also amplified the inward current evoked by supramillimolar K_o^+, in many cases fivefold and more (Table I). So the subsequent work was carried out in Ca^{2+}-MES buffered solutions at pH 5.5 or 6.1.

Ion Selectivity of the Inward Rectifier

An indication that the inward rectifying current is carried by K^+-selective channels in intact guard cells was drawn previously from its equilibrium or reversal potential

TABLE I

Steady-State Conductance of the K^+ Inward and Outward Rectifiers at pH 7.4 and 5.5

	pH	
	7.4	5.5
Inward rectifier		
$g_{K^+,-250}$, $mS\ cm^{-2}$	0.06 ± 0.02	0.42 ± 0.03
Outward rectifier		
$g_{K^+,-250}$, $mS\ cm^{-2}$	0.56 ± 0.04	0.44 ± 0.06

Data from 11 *Vicia* guard cells bathed in 10 mM KCl; buffers were 5 mM Ca^{2+}-HEPES, pH 7.4, and 5 mM Ca^{2+}-MES, pH 5.5. Steady-state conductance ($g_{K^+,-250} = I_{K^+}/(V - E_{K^+})$ for $V = -250$ mV [inward rectifier]) calculated from clamp cycles as shown in Fig. 1 after subtracting the instantaneous current component to obtain I_{K^+}. Outward rectifier conductance was obtained analogously on stepping from a conditioning voltage of −100 to +50 mV. Current reversal potentials (E_{K^+}) were determined from tail current relaxations (see also Blatt, 1988*a*).

(E_{rev}), which parallels E_{K^+} as the extracellular K^+ concentration is varied (Blatt et al., 1990*b*). The inward rectifier also discriminated among other alkali cations, as could be demonstrated in the present studies under equilibrium conditions. In this case, E_{rev} was determined under biionic conditions after substituting 10 mM of the cation (X) for K^+ in the bathing medium. Selectivities were derived from constant field assumptions and the shift in E_{rev}, so that the apparent selectivity (permeability) ratio was as follows:

$$P_{X^+}/P_{K^+} = \exp\,[zF(E_{rev,X} - E_{rev,K^+})/RT] \quad (1)$$

where $z = 1$ and F, R, and T have their usual meanings. The results are summarized in Table II and are consistent with the Eisenman series IV for binding interaction with a site in the channel pore of moderate to weak field strength (see Eisenman and Horn, 1983). Note that the equilibrium selectivities for K^+ over Na^+ and Cs^+ are rough estimates only; an inward current could be measured with Cs^+ in two cells, but only when the membrane was driven to voltages near −250 mV. No time-dependent inward current was recorded with 10 mM Na^+ in the bath, and free-running membrane potentials frequently exceeded (−)200 mV. Such high selectivities, as well as their relative ordering, contrast with results from guard cell protoplasts (Schroeder, 1988) and may reflect one consequence of plant protoplast isolation. (It

TABLE II

Cation Selectivity of the Inward Rectifier

	X			
	K^+	Rb^+	Cs^+	Na^+
P_X/P_{K^+}	1.0	0.21 ± 0.03	~0.03 (0.01–0.05)	<0.001

Data from five *Vicia* guard cells bathed in 10 mM chloride salts of each cation with 5 mM Ca^{2+}-MES, pH 6.1. Permeability ratios (P_X/P_{K^+}) were determined by Eq. 1.

is worth noting, too, that Na^+ [as well as Cs^+] is known to block current through several inward rectifying K^+ channels in animal preparations [cf. Ohmori, 1978; Standen and Stanfield, 1979). Although Na^+ failed to support a measurable current through the inward rectifier, no evidence could be found for block by Na_o^+ when added as the Cl^- (data not shown) and butyrate salts (cf. Fig. 13) at concentrations of 5–30 mM in the presence of 3–30 mM K_o^+.)

Based on the ability of the cation to carry current (permeate the channel), the inward rectifier also selected strongly against Rb^+. The data in Fig. 3 from one guard cell are typical. Substituting Rb^+ for K^+ displaced E_{rev} by −39 mV, consistent with a 5:1 selectivity, K^+:Rb^+; but the current tails and steady-state *I-V* curves indicated that, with equivalent driving forces, K^+ carried >20-fold the current recorded in Rb^+. The distinction, in this instance, lies in the ion–channel interaction assayed, and the data thus complement similar observations of channel behavior in animal cells (cf. Hille, 1973, 1984). It appears that Rb^+ can compete effectively under equilibrium conditions for binding site(s) within the channel, but permeates the channel pore only slowly.

Block of the Inward Rectifier by TEA and Neurotoxins

Block by K^+ channel antagonists provides a second line of evidence bearing on the origin of the guard cell K^+ current. As found previously with the guard cell outward rectifier, the inward rectifying K^+ current was also sensitive to tetraethylammonium chloride (TEA). Block by TEA was reversible and essentially voltage independent (Fig. 4), and at suboptimal concentrations TEA had no measurable effect on current activation or deactivation kinetics (not shown). Significantly higher concentrations of the channel blocker were required to achieve the same degree of block, however; whereas 10 mM TEA was sufficient to eliminate all measurable current through the outward rectifier (Blatt, 1988*a*), current through the inward rectifier was still evident in the presence of 30 mM TEA (Fig. 4). Titration of TEA block yielded an apparent $K_{1/2}$ of 9.1 mM in 10 mM K_o^+ (Fig. 4).

In addition to the effects of TEA, current through the inward rectifier responded to the neurotoxins α-dendrotoxin (DTX) and charybdotoxin (CTX). Data from one guard cell challenged with DTX are shown in Fig. 5; comparable results were obtained in experiments with four other cells and in three cells with CTX. A detailed study of toxin block was not undertaken; however, 50 nM of either toxin completely blocked the K^+ current and in neither case could the current be recovered, even after prolonged washing without toxin (Fig. 5).[2]

Voltage K^+ and Ca^{2+} Dependence of Inward Rectifier Current

Despite the clear alliance of the guard cell inward rectifier with the broad family of K^+ channels in biological membranes, there are indications that guard cell and possibly

[2] In one previous study of neurotoxin action on K^+ channels in *Chara*, channel block could not be resolved (Tester, 1988); however, both toxins are strongly basic polypeptides, which raises the question of toxin permeation through the *Chara* cell wall (see Tester, 1988). The point is all the more at issue because the measurements were carried out after prolonged exposures to La^{3+}, which might be expected to alter the charge on, and hence the ion exclusion and binding characteristics of the cell wall.

other higher plant K^+ channels diverge fundamentally from the established norms for channel gating (see Blatt, 1991*a*). Considerable evidence is now in hand showing that the inward rectifying K^+ channels of guard cells are *in*activated by micromolar intracellular Ca^{2+} concentrations (Schroeder and Hagiwara, 1989; Blatt et al., 1990*b*). Details are lacking, but guard cell K^+ channels may also be sensitive to extracellular Ca^{2+} (Busch et al., 1990). Furthermore, in preliminary work Schroeder (1988) suggested that gating of inward rectifying K^+ currents in guard cell protoplasts was

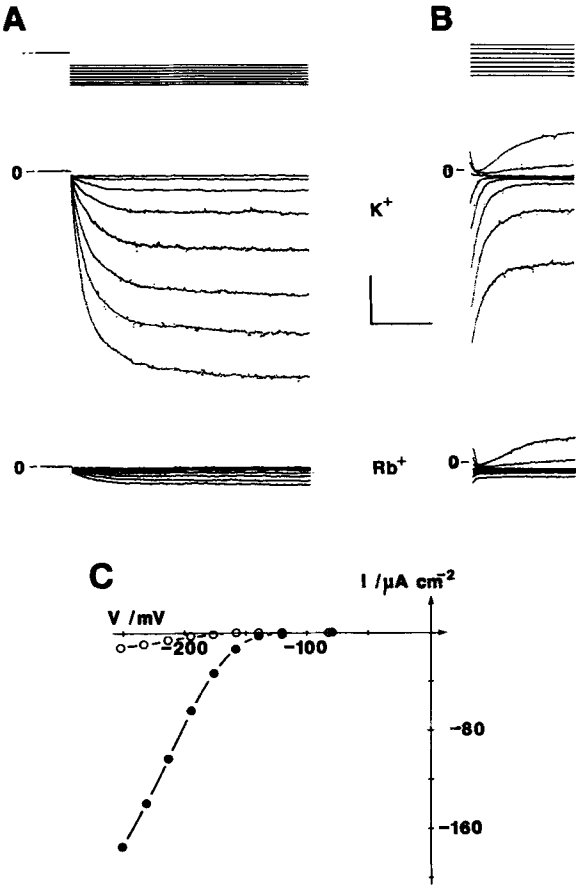

FIGURE 3. Cation selectivity as reflected in the conductance of the inward rectifier for K^+ and Rb^+. Data are from one *Vicia* guard cell bathed in 5 mM Ca^{2+}-MES, pH 5.5, and 10 mM KCl or 10 mM RbCl. Cell parameters: surface area, $1.9 \cdot 10^{-5}$ cm^2; volume, 4.9 pl; stomatal aperture, 9 μm. (*A*) Activation. Clamp parameters (eight cycles): conditioning voltage, −80 mV; test voltages, −120 to −250 mV. (*B*) Deactivation. Clamp parameters (eight cycles): conditioning voltage, −250 mV; test voltages, 0 to −200 mV. V_m (=holding voltage), −51 mV, both in K^+ and Rb^+. Scale: vertical, 40 μA cm^{-2} or 300 mV; horizontal, 200 ms. E_{rev}: −62 mV, K^+; −101 mV, Rb^+. (*C*) Steady-state *I-V* characteristics in K^+ (●) and Rb^+ (○) from *A* after subtracting instantaneous currents. As determined from the conductance ratios, g_{Rb+}/g_{K+} over the voltage range −250 to −200 mV, the mean selectivity from this and three additional cells was 0.06 ± 0.02.

insensitive to K_o^+ concentration, in stark contrast to the classic inward rectifiers of muscle and egg cell membranes (cf. Hagiwara et al., 1976, 1978).

To assess the effects of voltage and extracellular cation concentrations, inward rectifier current was recorded, using two-step protocols, to determine the conductance–voltage characteristics and to detail the kinetics for voltage-dependent current activation and deactivation. Inward rectifier conductance (g_{K^+}) was taken from the slopes of instantaneous *I-V* curves, recorded after clamp steps to one of several

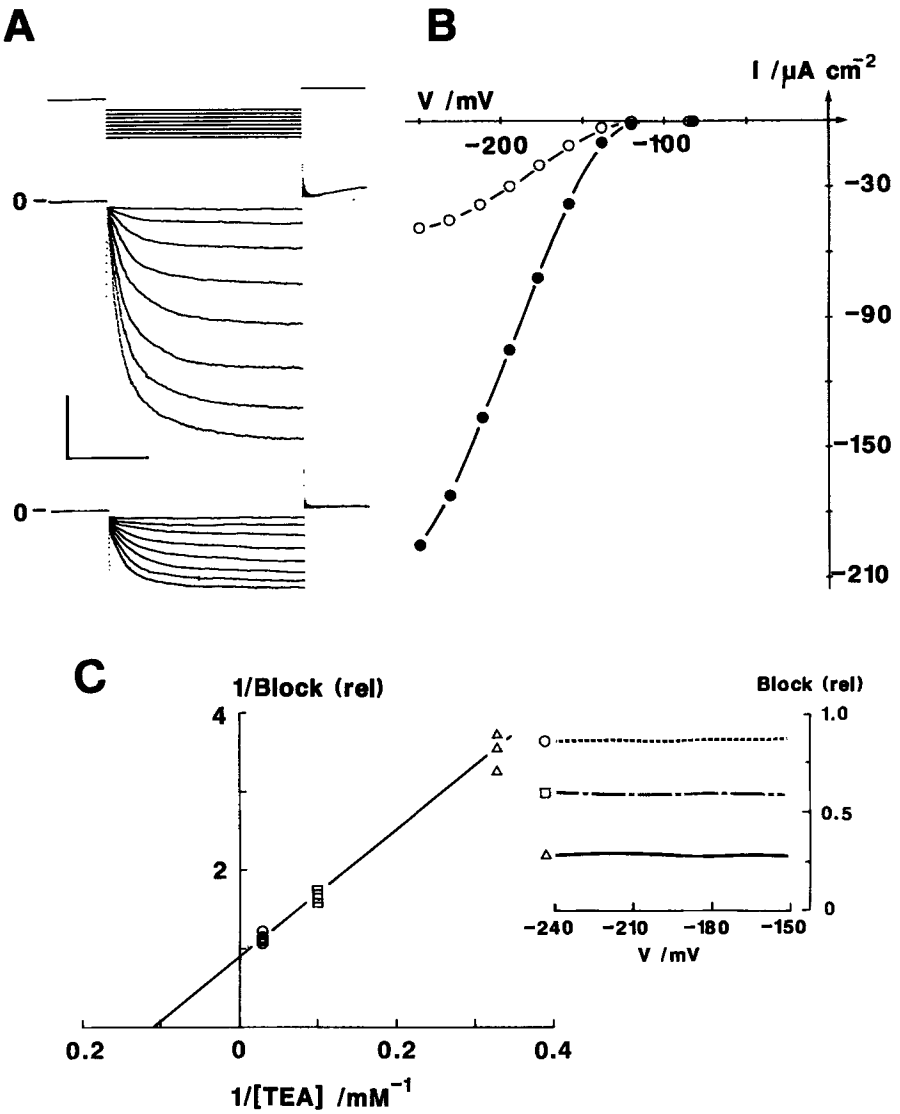

FIGURE 4. Inward rectifier block by TEA. Data from one *Vicia* guard cell bathed in 5 mM Ca^{2+}-MES, pH 6.1, and 10 mM KCl; data from three additional cells are included in *C*. Cell parameters: surface area, $1.6 \cdot 10^{-5}$ cm^2; volume, 3.6 pl; stomatal aperture, 6 μm. (*A*) Current activation and deactivation before (center) and after (below) adding 10 mM TEA to the bath. Clamp protocol (above, eight cycles): conditioning voltage, −80 mV; test voltages, −120 to −250 mV; tailing voltage, −30 mV. Holding potentials (=V_m): control, −48 mV; +TEA, −42 mV. Scale: vertical, 60 μA cm^{-2} or 300 mV; horizontal, 500 ms. (*B*) Steady-state *I-V* characteristics derived from *A* (cross-referenced by symbol) after subtracting the instantaneous currents. (*C*) Double-reciprocal plot of relative current block as a function of TEA concentration for four cells, including the data in *A* and *B*. The apparent $K_{1/2}$ for TEA in 10 mM K_o^+ is 9.1 mM. (*Inset*) Voltage dependence of TEA block calculated as $1 - I_{K^+,+TEA}/I_{K^+,contrl}$ for 3, 10, and 30 mM TEA for the data in *A* and *B*.

conditioning voltages, and measurements were repeated in each cell over a range of K_o^+ concentrations. The current was observed only twice at 1 mM K_o^+ ($n = 42$) and on no occasion below (0.5 and 0.1 mM) this concentration; however, instantaneous *I-V* curves were roughly linear over the concentration range 3–30 mM K_o^+ (see Fig. 8; also Blatt et al., 1990*b*), so the conductance could be estimated as

$$g_{K^+} = I_{K^+}/(V - E_{K^+}) \tag{2}$$

where I_{K^+} is the K^+ current at clamp voltage V after subtracting the leak current.

Fig. 6 illustrates the $g_{K^+} - V$ relations of the inward rectifier from one guard cell in 3, 10, and 30 mM K_o^+. The data highlight the strong dependence of gating on membrane voltage and confirm its insensitivity to the cation concentration outside

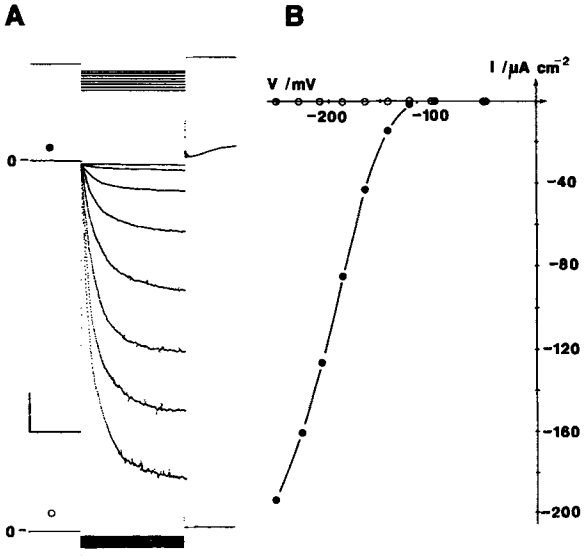

FIGURE 5. Inward rectifier block by 50 nM α-dentrotoxin (DTX). Data from one *Vicia* guard cell bathed in 5 mM Ca^{2+}-HEPES, pH 6.1, and 30 mM KCl. Cell parameters: surface area, $1.8 \cdot 10^{-5}$ cm^2; volume, 4.7 pl; stomatal aperture, 7 μm. (*A*) Activation and deactivation before (●) and 3 min after (○) perfusing with DTX, with zero current levels indicated. Clamp protocol (above, eight cycles): conditioning voltage, −50 mV; test voltages, −100 to −250 mV; tailing voltage, 0 mV. Holding potential ($=V_m$), −38 mV (−DTX) and −33 mV (+DTX). Scale: vertical, 30 μA cm^{-2} or 300 mV; horizontal, 500 ms. (*B*) Steady-state $I_{K^+} - V$ characteristics from *A* (cross-referenced by symbol) after subtracting the corresponding instantaneous currents.

(Schroeder, 1988). Steady-state conductance rose with increasing (negative) voltage from −120 mV to a maximum at voltages beyond approximately −230 mV; conductance at any one voltage increased with K_o^+, roughly in proportion to the square root of the cation concentration. Qualitatively similar dependencies of $g_{K^+,max}$ on K_o^+ have been described for inward rectifiers in tunicate eggs (cf. Hagiwara and Yoshii, 1979). But unlike inward rectifiers in these preparations, the guard cell K^+ current rose in scalar fashion with K_o^+, that is, without an appreciable change in the clamp voltage required to achieve half-maximal g_{K^+} (Fig. 6, arrowheads).

For a quantitative indication of the relative sensitivities to voltage and K_o^+, $g_{K^+} - V$ curves were fitted to a Boltzmann function of the conditioning voltage, V, such that

$$g_{K^+} = g_{K^+,max}/(1 + e^{\delta F(V_{1/2} - V)/RT}) \tag{3}$$

where $g_{K^+,max}$ is the maximum conductance at saturating negative voltages, $V_{1/2}$ is the voltage at which $g_{K^+} = 0.5 \cdot g_{K^+,max}$, and δ is the (minimum) charge moved within the membrane electric field during gating. The $g_{K^+} - V$ characteristics at the three K_o^+ concentrations in Fig. 6 were fitted jointly to Eq. 3 while holding δ and $V_{1/2}$ in common between data sets, and yielded values for these two parameters of 1.4 and −183 mV, respectively. When each curve was fitted separately, values for δ ranged from 1.3 to 1.55 and for $V_{1/2}$ from −181 mV to −192 mV, but the variations were not statistically significant. Comparable results were obtained from four other cells, and are summarized in Table III.

The same conclusion was drawn from the macroscopic current kinetics. The voltage dependencies for current activation and deactivation in four cells at the three K_o^+ concentrations are pooled in Table III. Activation was characterized from currents

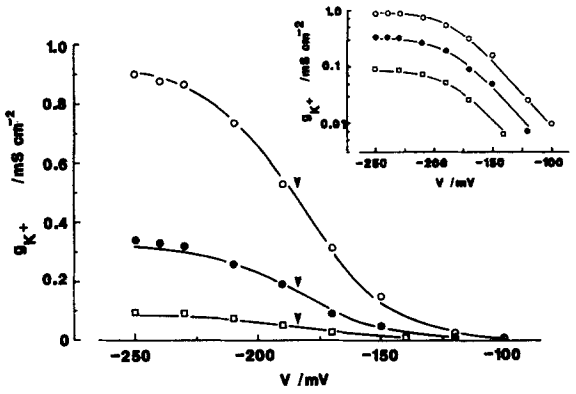

FIGURE 6. Inward rectifier conductance (g_{K^+}) as a function of extracellular K^+ concentration. Data from one *Vicia* guard cell bathed in 5 mM Ca^{2+}-MES, pH 6.1, with 3 (□), 10 (●), and 30 mM (○) KCl. Cell parameters: surface area, $1.5 \cdot 10^{-5}$ cm^2; volume, 3.2 pl; stomatal aperture, 8 μm. Conductances were determined using a two-step protocol from the instantaneous currents recorded at voltages between 0 and −200 mV after 800-ms conditioning steps at the voltages indicated. Instantaneous currents were well fitted to a linear function of voltage in all cases, and background conductances were subtracted from the fitted slopes. Background conductances were determined in similar two-step protocols, but after conditioning steps at −100, −80, and −50 mV for 3, 10, and 30 mM K_o^+, respectively. Shown are the results of joint fitting to the Boltzmann function (Eq. 3) yielding δ = 1.4 and $V_{1/2}$ = −183 mV (arrowheads). Fitted $g_{K^+,max}$: 0.087 mS cm^{-2} (□); 0.32 mS cm^{-2} (●); 0.92 mS cm^{-2} (○). See text and Table III for additional details. (*Inset*) Data and fitting replotted with g_{K^+} on a logarithmic scale.

registered on stepping the clamp voltage from values between −50 and −100 mV to voltages negative of −120 mV, and half-times for activation taken directly from the time-dependent current component; current trajectories during deactivation were well-fitted to a simple exponential function of time (see Fig. 8, *inset*). Both activation and deactivation showed appreciable voltage sensitivities. Activation half-times and the time constant, τ, for deactivation increased e-fold per +191 and −43 mV, respectively, with τ approaching a minimum of ~8 ms near 0 mV. However, neither parameter showed a significant dependence on K_o^+ at concentrations from 3 to 30 mM.

Extracellular Ca^{2+}, too, proved largely ineffectual in modifying the conductance and kinetic characteristics of the inward rectifier, in contrast to its action on the channels from the cytoplasmic side of the membrane (cf. Schroeder and Hagiwara,

TABLE III

Activation, Deactivation, and Steady-State Conductance Characteristics of the Inward Rectifier in 3, 10, and 30 mM K_0^+

	K_0^+ (mM)		
	3	10	30
δ	1.43 ± 0.05	1.38 ± 0.06	1.39 ± 0.03
$V_{1/2}$, *mV*	−186 ± 3	−188 ± 4	−187 ± 2
Activation			
$t_{1/2}$ (−200 mV), *ms*	168 ± 6	164 ± 7	167 ± 3
$t_{1/2}$ (−250 mV), *ms*	122 ± 4	119 ± 5	125 ± 3
Deactivation			
τ (−120 mV), *ms*	69 ± 5	65 ± 4	64 ± 4
τ (0 mV), *ms*	—	8 ± 1	8 ± 1

Data from five *Vicia* guard cells (four for activation/deactivation data) bathed in 5 mM Ca^{2+}-MES, pH 6.1, with 3, 10, and 30 mM KCl. Apparent gating charge (δ) and half-maximal gating voltage ($V_{1/2}$) determined from separate fittings to the Boltzmann function, Eq. 3. Activation half-times ($t_{1/2}$) were taken directly from the time-dependent current records (see Fig. 1); 500-ms conditioning steps were at −100, −80, and −50 mV for 3, 10, and 30 mM K_0^+, respectively. Time constants (τ) for deactivation were determined from single exponential fittings of the current relaxations after conditioning steps to −250 mV (see also Fig. 8).

1989; Blatt et al., 1990*b*) and, at least for $[Ca^{2+}]_o \leq 1$ mM, inward rectifier behavior could be understood in the context of charge screening at the membrane surface (see Hille et al., 1975; Hille, 1984; and Discussion in this paper). Figs. 7 and 8 show the results of conductance and half-time analyses from one cell bathed in 0.1 and 1 mM Ca^{2+} media and additional data are summarized in Table IV. Raising Ca_o^{2+} over this concentration range shifted the conductance characteristic (Fig. 7) to the right along the voltage axis, but with a symmetric displacement of activation and deactivation kinetic characteristics (Fig. 8). Extracellular Ca^{2+} had no impact on the apparent gating charge δ, and only marginal declines in $g_{K^+,max}$ were observed in 1 mM Ca_o^{2+}. A further rise to 10 mM Ca_o^{2+} was observed to depress inward rectifier conductance (60–80% relative to 1 mM Ca_o^{2+}) and to shift the conductance characteristic left (≤ -14 mV) along the voltage axis (not shown). This latter response parallels that of intracellular Ca^{2+} (Schroeder and Hagiwara, 1989; Blatt et al., 1990*b*) and may reflect

TABLE IV

Steady-State Conductance Characteristics of the Inward Rectifier in 0.1 and 1.0 mM Ca_0^{2+}

	Ca_0^{2+} (mM)	
	0.1	1.0
δ	1.35 ± 0.04	1.37 ± 0.02
$V_{1/2}$, *mV*	−221 ± 5	−188 ± 3

Data from four *Vicia* guard cells bathed in 5 mM Na^+-MES, pH 6.1, and 30 mM KCl, with 0.1 and 1.0 mM $CaCl_2$. Apparent gating charge (δ) and half-maximal gating voltage ($V_{1/2}$) were determined from separate fittings to the Boltzmann function, Eq. 3.

an extracellular Ca^{2+} load sufficient to raise steady-state free Ca^{2+} levels in the cytosol (cf. Busch et al., 1990).

H^+ Permeation and pH Dependence of the Inward Rectifier

Although the requirement for millimolar K_o^+ would seem to militate against the idea, the pH dependence outlined above could indicate a significant permeability to H^+ and it was important to examine this possibility. High H^+ conductances have been described for the chloroplast CF_0 "porin" (Wagner et al., 1989) and a H^+ conductance (channel) is well-known in *Chara* (see Beilby, 1990). However, no evidence

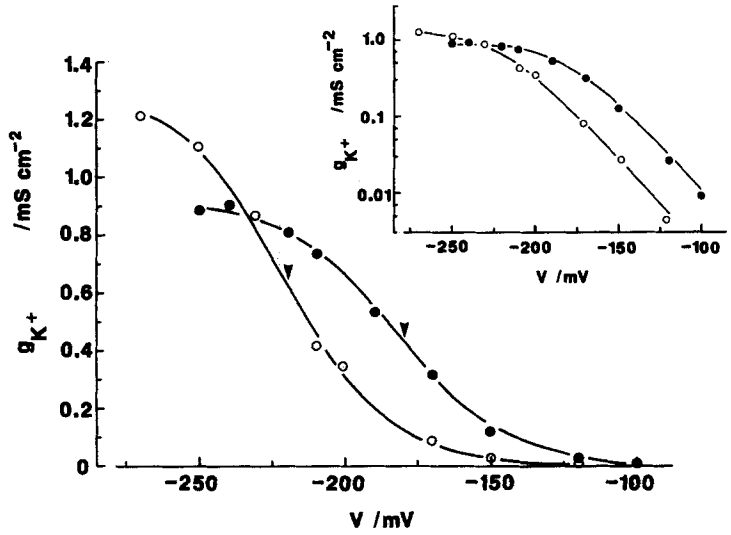

FIGURE 7. Inward rectifier conductance (g_{K^+}) as a function of extracellular Ca^{2+} concentration. Data from one *Vicia* guard cell bathed in 5 mM K^+-MES and 28 mM KCl ($[K^+]$ = 30 mM), pH 6.1, with 0.1 (○) and 1.0 mM (●) $CaCl_2$. Cell parameters: surface area, $1.6 \cdot 10^{-5}$ cm^2; volume, 4.9 pl; stomatal aperture, 8 μm. Steady-state conductance determined from instantaneous currents recorded using the two-step protocol of Fig. 6. The curves are joint fittings to Eq. 3 with δ held in common. Fitted parameters, 0.1 mM Ca_o^{2+}: $g_{K^+,max}$, 1.33 mS cm^{-2}; $V_{1/2}$, −217 mV. 1.0 mM Ca_o^{2+}: $g_{K^+,max}$, 0.93 mS cm^{-2}; $V_{1/2}$, −183 mV. The apparent gating charge, δ = 1.35. (*Inset*) Data and fitting replotted with g_{K^+} on a logarithmic scale.

could be found for inward rectifier current carried by H^+. Reversal potentials for the K^+ current were insensitive to pH_o over the range 7.4–5.5 (Table V), and even at pH 5.5 no current was detectable when K_o^+ was reduced below 1 mM (see above). These observations in no way rule out H^+ permeation through the inward rectifier (at pH_o 5.5 the $[H^+]_o$ was roughly three orders of magnitude below the K_o^+ concentrations that gave a measurable current); rather, the extreme pH sensitivity of the current highlights a regulatory effect of H^+ on the K^+ channel current.

To characterize the nature of this pH sensitivity further, inward rectifier current was recorded, using two-step protocols, to assess the influence of pH_o on the steady-state g_{K^+}-V characteristic and on the kinetics for voltage-dependent current

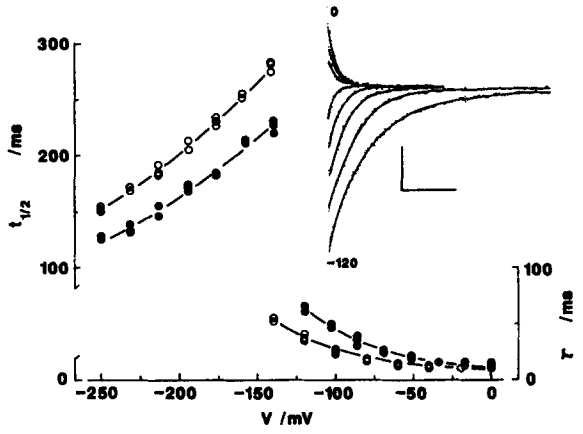

FIGURE 8. Ca^{2+} dependence of inward rectifier activation and deactivation kinetics. Data from three *Vicia* guard cells, including the cell in Fig. 7; conditions are the same as in Fig. 7 with the cell bathed in 0.1 mM (○) and 1.0 mM (●) Ca_o^{2+}. Each point is the mean of at least two measurements. Activation half-times ($t_{1/2}$; left-most data set) were taken directly from the time-dependent current records (see Fig. 1) after 500-ms conditioning steps at −50 mV. Time constants (τ; right-most data set) for deactivation were determined from single exponential fittings of the current relaxations after conditioning steps to −250 mV (see inset). Curves for activation and deactivation are empirical and, in each case, are joint fittings between the two Ca^{2+} concentrations to a simple exponential function with a common exponent; the fittings yielded an *e*-fold rise in $t_{1/2}$ per +178 mV, and in τ per −45.4 mV, with activation and deactivation curves shifted +33 mV between 0.1 and 1.0 mM Ca_o^{2+}. τ approached a minimum of 7.4 ms at positive voltages.

activation and deactivation. As before, current kinetics were recorded after clamp steps to one of several conditioning voltages, and inward rectifier conductance (g_{K^+}) was taken from the slopes of the instantaneous *I-V* curves (Eq. 2). Measurements were carried out in 10 and 30 mM K_o^+ while stepping the bath pH between values ranging from 8.1 to 5.5. Because a set of eight pulse cycles required > 1 min to complete and log, these records were generally interspersed with steady-state *I-V* scans, assayed using a bipolar staircase protocol and run at intervals throughout the experiments.

Results from one cell repeatedly challenged with pH steps between 7.4, 6.1, and 5.5 in the presence of 10 mM K_o^+ are shown in Fig. 9. Transfers to acid pH gave the characteristic rise in steady-state current through the inward rectifier, which was fully reversible on returning to pH_o 7.4 and was essentially complete within the exchange time of the bath. Note, by contrast, that current through the outward rectifier was largely unaffected by pH_o. Only at pH_o 5.5 was this current depressed in the steady

TABLE V

Reversal Potential of the Inward Rectifier at pH 7.4 and 5.5

	pH	
	7.4	5.5
E_{rev}, *mV*	−71 ± 4	−74 ± 5
ΔE_{rev}, *mV*	0 ± 1	

Data from 11 *Vicia* guard cells bathed in 10 mM KCl; buffers were 5 mM Ca^{2+}-HEPES, pH 7.4, and Ca^{2+}-MES, pH 5.5. Reversal potentials (E_{rev}) were determined by interpolation of tail current relaxations. ΔE_{rev} is the difference in reversal potentials at the two pH_o values and was determined on a cell-by-cell basis.

state, and then in an apparently voltage-independent manner; no significant change could be detected in the time course for activation in three cells (data not shown).

Raising the extracellular H^+ concentration also had a profound effect on the steady-state conductance characteristic for the inward rectifier and on its activation kinetics. Data gathered over the entire pH range from one cell are shown in Figs. 10 and 11. Raising $[H^+]_o$ affected the $g_{K^+} - V$ profile in a manner antiparallel with pCa_i, i.e., analogous to lowering the intracellular free Ca^{2+} concentration (see Schroeder and Hagiwara, 1989; Blatt et al., 1990*b*); acid pH shifted $V_{1/2}$ to the right (positive-going) along the voltage axis and increased $g_{K^+,max}$ to a maximum near pH_o 5.5. The

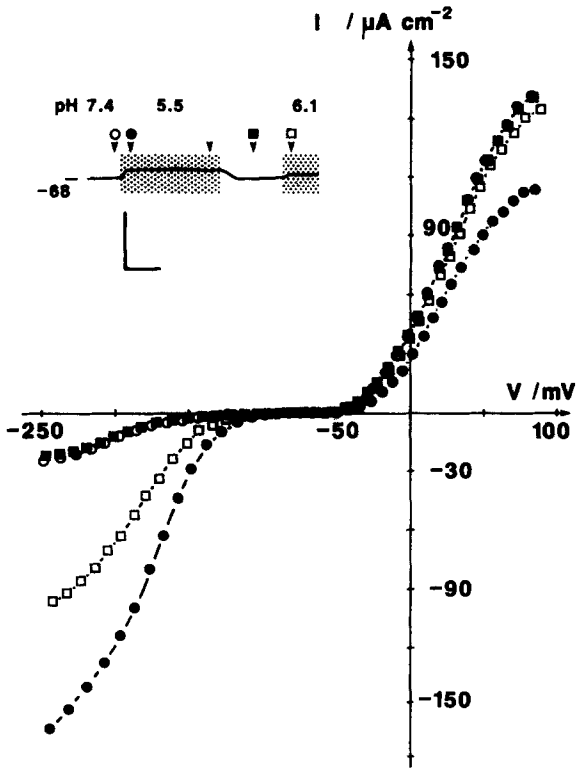

FIGURE 9. Steady-state K^+ current response to extracellular pH. Data from one *Vicia* guard cell bathed in 10 mM KCl plus 1 mM $CaCl_2$ and gathered using a bipolar staircase protocol (pulse duration, 500 ms). Buffers were 5 mM Na^+-HEPES, pH 7.4 (○, ■) and 5 mM Na^+-MES, pH 6.1 (□) or pH 5.5 (●). Cell parameters: surface area, $1.8 \cdot 10^{-5}$ cm^2; volume, 4.7 pl; stomatal aperture, 9 µm. (*Inset*) Voltage trace with times of *I-V* scans (masked from trace) marked by carats and cross-referenced by symbol to the *I-V* curves. Shading indicates exposure periods to acid pH_o (values indicated above). Scale: vertical, 40 mV; horizontal, 2 min. Data gathered at the end of the pH_o 5.5 exposure are not shown, but superimpose on the *I-V* data shown for this pH_o. Note the limited pH_o sensitivity of the outward rectifying (K^+ channel) current.

cumulative results from 11 cells over this pH range gave a mean shift (acid-going) in $V_{1/2}$ of +21 ± 2 mV/pH unit (see also Fig. 10). At any one clamp voltage, acid pH also accelerated the activation of the inward rectifier and slowed its deactivation (Fig. 11 and Table VI); unlike inward rectifier response to Ca_o^{2+}, however, this effect showed a distinct asymmetry, with a bias to accelerating current activation.

The most pronounced effects evident in Figs. 10 and 11 occurred over a relatively narrow pH range near neutrality. Replotting the conductances in Fig. 10 as a function of pH shows that, at any one voltage, the conductance saturated with respect to pH at micromolar H^+ concentrations (Fig. 12). At each voltage, g_{K^+} was well-fitted

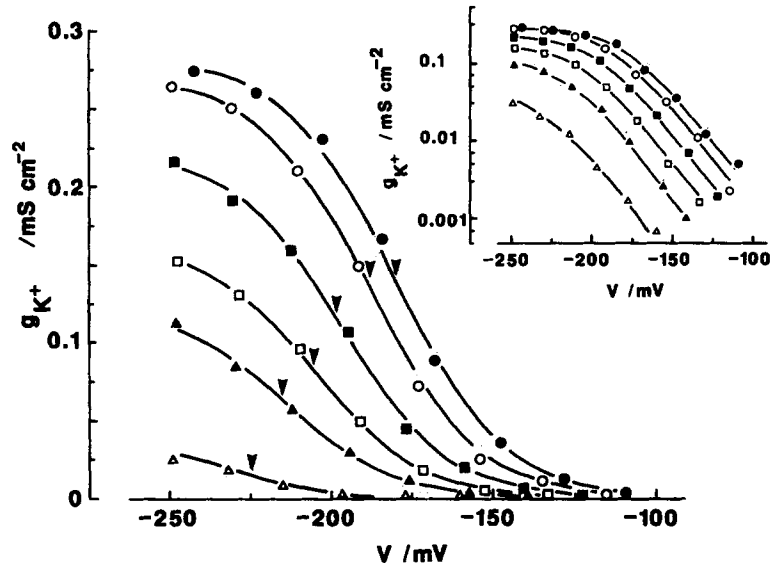

FIGURE 10. Inward rectifier conductance as a function of voltage over the pH range 5.5–8.1. Data from one *Vicia* guard cell bathed in 10 mM KCl and 1 mM $CaCl_2$ at pH 5.5 (●), 6.1 (○), 6.5 (■), 7.0 (□), 7.4 (▲), and 8.1 (△). Buffers were 5 mM TAPS (pH 8.1), HEPES (pH 7.4 and 7.0), and MES (pH 6.5, 6.1, and 5.5) titrated with NaOH. Cell parameters: surface area, $1.8 \cdot 10^{-5}$ cm^2; volume, 4.0 pl; stomatal aperture, 13 μm. Steady-state conductance determined from instantaneous currents recorded using a two-step protocol, with instantaneous currents recorded at voltages between 0 and −200 mV after 800-ms conditioning steps at the voltages indicated. Comparable results were also obtained from steady-state (bipolar staircase) recordings (cf. Fig. 9). Instantaneous currents were fitted to a linear function of voltage (Eq. 2) and background conductances were subtracted. The curves are joint fittings to the Boltzmann function (Eq. 3) with the gating charge, δ, held in common. Fitted parameters: δ (common), 1.55; pH-dependent parameters,

pH	5.5	6.1	6.5	7.0	7.4	8.1
$V_{1/2}$, mV	−179	−188	−198	−206	−214	−224
$g_{K^+,max}$, mS cm^{-2}	0.28	0.27	0.22	0.17	0.11	0.023

(*Inset*) Data and fitting replotted with g_{K^+} on a logarithmic scale.

by the Henderson-Hasselbalch equation of the form

$$(g_{K^+,max} - g_{K^+})/g_{K^+,max} = 10^{pH-pK_a} \quad (4)$$

Significantly, the pK_a for K^+ inward rectifier conductance itself showed an appreciable voltage dependence. Results of the fittings in Fig. 12 and of data from four additional cells are summarized in the inset, and yield an apparent *e*-fold rise in binding affinity ($=10^{-pK_a}$) per (−)38-mV increase in electrical driving force across the membrane. In effect, the current followed pH as if H^+ bound at a single, titratable site and H^+ binding was itself sensitive to membrane voltage.

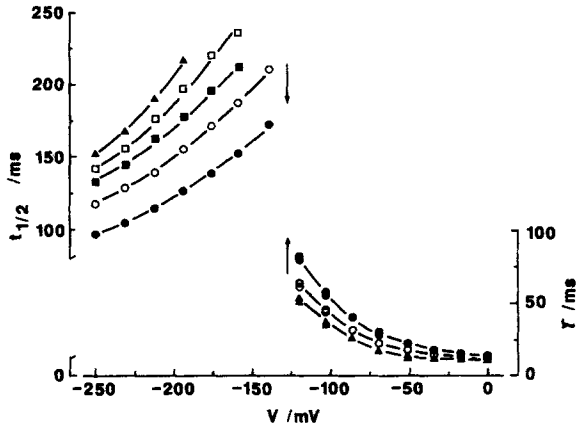

FIGURE 11. pH dependence of inward rectifier activation and deactivation kinetics. Data from one *Vicia* guard cell with conditions the same as in Fig. 10. Cell parameters: surface area, $2.0 \cdot 10^{-5}$ cm^2; volume, 5.2 pl; stomatal aperture, 10 μm. Each point is the mean of at least two measurements. Activation half-times ($t_{1/2}$; left-most data set) were taken directly from the time-dependent current records (see Figs. 1 and 13) after 500-ms conditioning steps to −80 mV. Time constants (τ; right-most data set) for deactivation were determined from single exponential fittings of the current relaxations after 800-ms conditioning steps to −250 mV. Bath pH was 5.5 (●), 6.1 (○), 6.5 (■), 7.0 (□), and 7.4 (▲). The arrows (center) are visual guides to the overall shift with acid-going pH. Curves for activation and deactivation are empirical and, in each case, are joint fittings between the pH values to a simple exponential function with a common exponent; the fittings yield an *e*-fold rise in $t_{1/2}$ per +174 mV, and in τ per −45.8 mV. τ approaches a minimum of 7.8 ms at positive voltages.

Influence of pH_i

Overall, the data outlined above are consistent with H^+ acting on the K^+ channels from the outside. Nonetheless, the possibility remains that acid pH_o could trigger, within the cell, additional metabolic events intermediate to the effects ultimately observed on inward rectifier current and gating. One consequence of lowering pH_o around plant and fungal cells is to impose a parallel, if much attenuated acid load intracellularly (Sanders and Slayman, 1982; Felle, 1988*b*). Significantly, pH_i often lags only a few tens of seconds behind pH_o in these instances. The repercussions are likely to extend also to homeostatic control of cytoplasmic free Ca^{2+} concentrations (see Moody, 1984; Kurkdjian and Guern, 1989). So the pH sensitivity of the inward

TABLE VI

Effect of pH on Inward Rectifier Activation and Deactivation Kinetics

	pH_o	
	7.4	5.5
Activation		
$t_{1/2}$ (−250 mV), *ms*	158 ± 6	96 ± 4
Deactivation		
τ (−120 mV), *ms*	56 ± 3	88 ± 3
τ (0 mV), *ms*	7.9 ± 0.1	7.8 ± 0.1

Data from 11 *Vicia* guard cells bathed in 10 mM KCl. Buffers were 5 mM Ca^{2+}-HEPES, pH 7.4, and Ca^{2+}-MES, pH 5.5. Activation half-times ($t_{1/2}$) and deactivation time constants (τ) were determined in two-step clamp protocols (see also Table III).

rectifier could depend, not on extracellular, but on intracellular pH and possibly in conjunction with pCa_i (see Felle, 1988*a*; Blatt, 1991*a*).

Selecting between these two alternatives, (*a*) of a direct effect of pH_o and (*b*) of a secondary effect mediated by pH_i, requires that intracellular pH be manipulated independently of pH_o. To this end, cytoplasmic acid loads may be imposed using weak acids which, in the undissociated form, permeate the membrane freely. The internal concentration of the acid anion (and H^+ load) can be calculated from the Henderson-Hasselbalch equation (above; see also Waddell and Bates, 1969), assuming that the free acid equilibrates across the plasma membrane and provided that pH_o, pH_i, and the pK_a of the acid are known. Recent measurements of the cytoplasmic pH for guard cells place the figure near 8.0 (Baier and Hartung, 1988), and in line with best estimates for plants and fungi generally (Sanders and Slayman, 1982; Felle, 1988*b*; Kurkdjian and Guern, 1989). So, to a first approximation, a H^+

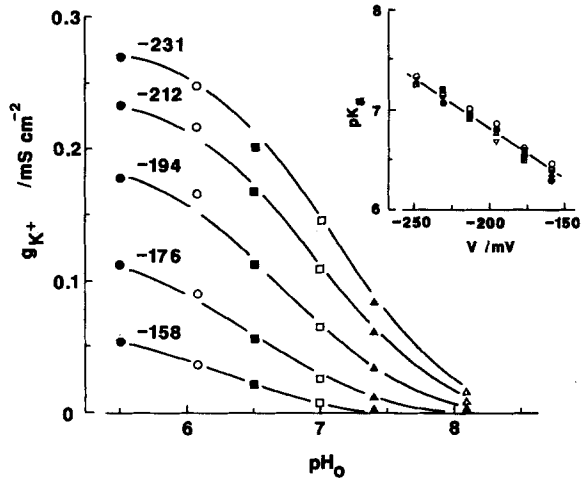

FIGURE 12. Inward rectifier conductance as a function of pH at voltages between −150 and −250 mV. Data from Fig. 10 replotted at the voltages indicated and fitted to the Henderson-Hasselbalch equation (Eq. 4). (*Inset*) pK_a values for pH-dependent activation as a function of voltage. Symbols are for the fittings shown (●) and for similar analyses of data from four other cells. The line was fitted by eye.

load equivalent to 30-fold the free acid concentration (and close to the total acid concentration) in the bath can be expected on adding a weak acid such as butyrate (pK_a 4.81) at pH_o 6.5.

For purposes of these studies, precise knowledge of the acid load was not important. Instead, current through the inward rectifier was monitored as before, and these records were compared against contiguous measurements of current through the outward rectifying K^+ channels as a check on the efficacy of acid loading. Measurements were carried out with 3, 10, and 30 mM Na^+-butyrate at pH_o 6.5 and in the presence of 10 mM K_o^+ in six separate experiments. In every case, 10 or 30 mM butyrate was required to elicit any response and the current recovered on washing out the weak acid. In every case, too, the effect of acid loading was restricted to the outward rectifier and the characteristics of the inward rectifier remained virtually unaltered.[3]

[3] An effect of the butyrate anion could be discounted. Quantitatively comparable currents through both K^+ channels were observed regardless of whether microelectrodes were filled with, and hence leaked (Blatt, 1987*a*), K^+-acetate or K^+-butyrate, pH 7.3 (not shown).

Data from one guard cell are summarized in Fig. 13 and illustrate the full extent of the inward rectifier response. Outward rectifier current was depressed to ~90% in 10 mM, and to <9% of the control in 30 mM butyrate; by contrast, steady-state current through the inward rectifier showed only marginal enhancement (<120% of the control) at the highest weak acid concentration. Even then, no appreciable shift was evident in the steady-state *I-V* profile for the inward rectifier, nor in its activation kinetics or its $g_{K^+} - V$ characteristic. Note that, for the outward rectifier, the effect of imposing a moderate acid load inside compares favorably to that of lowering pH_o to 5.5 (see Fig. 9). It appears, therefore, that the pH sensitivity of the inward rectifier cannot be a consequence of variations in pH_i, and must be ascribed to H^+ acting from outside the guard cell.

DISCUSSION

pH and K^+ Channel Activation

The activation of K^+ channels by extracellular H^+ represents a new departure in understanding the controls on ion channel activity in plant cells and, along with complementary data bearing on channel gating and block, sets the K^+ current apart from other inward rectifiers known in animal cells. Three key lines of evidence support the idea of pH_o control for the K^+ inward rectifier of *Vicia* stomatal guard cells. (*1*) Current activation saturates with respect to $[H^+]_o$, consistent with high-affinity binding of H^+ at a single, titratable site (Figs. 10–12). (*2*) Inward rectifier current appears largely insensitive to pH_i (Fig. 13). (*3*) Variations in pH do not affect the thermodynamic load on the current, as reflected in its reversal potential (Table V). The latter point carries particular weight for the guard cells, especially in light of earlier confusion about the relevant driving forces for K^+ uptake through the inward rectifier (Hedrich and Schroeder, 1989). Plant and fungal membranes are geared to a H^+ transport economy which, at least in *Neurospora,* is known to include H^+-coupled K^+ uptake (Rodriguez-Navarro et al., 1986). Following the *Neurospora* model, transport of K^+ coupled 1:1 with H^+ could be expected to show roughly a +60-mV shift in equilibrium (reversal) potential with a 100-fold rise in $[H^+]_o$ (lowering pH_o from 7.5 to 5.5). Clearly, this does not hold for the K^+ current in the present case, and a direct link to the H^+ circuit of the guard cell plasma membrane can be discounted.

Nor are the data consistent with charge screening as a primary mechanism of action for pH_o. In the simplest sense, charge screening alters the electric field within the membrane by compensating fixed charges at the membrane surface (see Hille et al., 1975; Hille 1984). The effect is to displace the electric field sensed by a channel (within the membrane) relative to the potential difference recorded between bulk solutions; but in all other respects channel current and gating should be unaffected unless the screening ion interacts with the channel itself. The inward rectifier response to Ca^{2+} follows this pattern, at least for low $[Ca^{2+}]_o$; the principle effect of raising $[Ca^{2+}]_o$ was to shift the gating characteristic and kinetics symmetrically to the right along the voltage axis (Figs. 7 and 8). Quite a different pattern was observed in the current response to pH_o. Indeed, there is good reason to suspect that H^+ acts on K^+ channel gating. External pH affected the K^+ current in its magnitude, instanta-

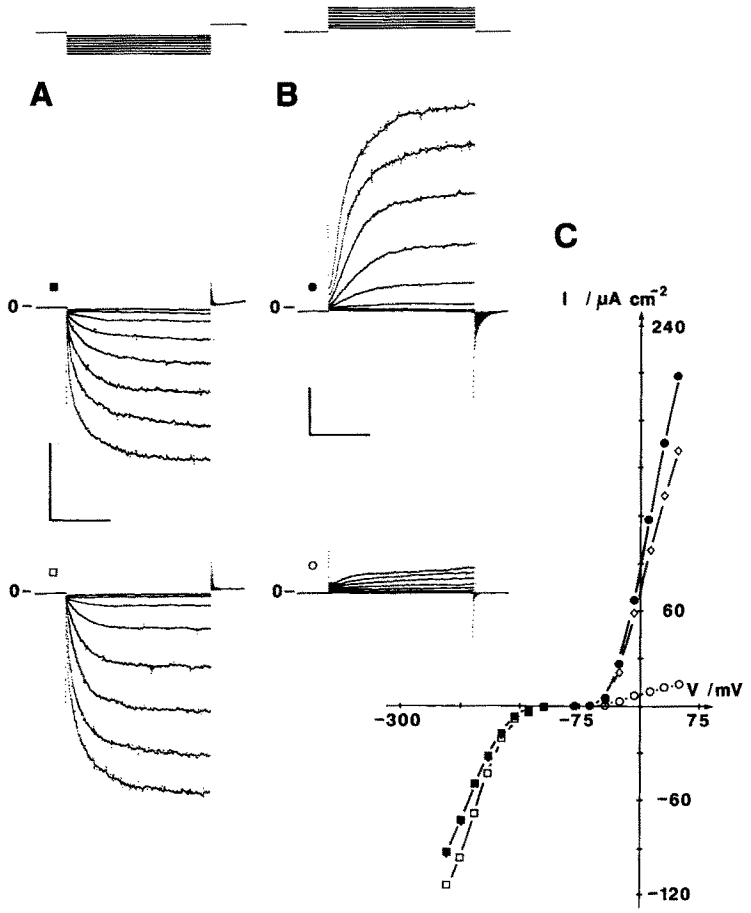

FIGURE 13. Inward and outward rectifier sensitivity to intracellular acid loads. Data from one *Vicia* guard cell bathed in Ca^{2+}-MES, pH 6.5, with 10 mM KCl (●, ■) and with butyrate added to a final concentration of 10 mM (◆, ◇) and 30 mM (○, □) after titrating to pH 6.5 with NaOH. Cell parameters: surface area, $1.8 \cdot 10^{-5}$ cm^2; volume, 4.8 pl; stomatal aperture, 10 μm. (*A*) Inward rectifier current before (■) and after (□) adding 30 mM butyrate. Zero current level as indicated. Clamp protocol (above, eight cycles): conditioning voltage, −100 mV; test voltages, −120 to −250 mV; tailing voltage, −50 mV. Holding potential ($=V_m$), −58 mV. Scale: vertical, 50 μA cm^{-2} or 500 mV; horizontal, 500 ms. (*B*) Outward rectifier current before (●) and after (○) adding 30 mM butyrate. Zero current level as indicated. Clamp protocol (above, eight cycles): conditioning voltage, −100 mV; test voltages, −75 to +50 mV; tailing voltage, −100 mV. Holding potential ($=V_m$), −54 mV. Scale: vertical, 50 μA cm^{-2} or 300 mV; horizontal, 500 ms. (*C*) Steady-state *I-V* curves for the inward and outward rectifying K^+ currents in *A* and *B* (cross-referenced by symbol). Additional data gathered in 10 mM butyrate (◆, ◇) are included.

neous conductance characteristics, and kinetics (Figs. 9–12), the effect of H^+ in the latter case being asymmetric and most pronounced in the kinetics for current activation (Fig. 11). Simply altering the number of channels available or their conductance would not give rise to such behavior. So again, the effect of pH on the K^+ current is more easily understood in terms of a direct interaction between H^+ and the channel protein(s).

How do external protons alter K^+ channel current? One additional observation is that the K^+ current saturated with respect to pH_o and voltage, such that increasing the electrical driving force (−)38 mV to draw H^+ into the membrane was equivalent in its effect to an *e*-fold rise in $[H^+]_o$ (Figs. 10 and 12). The simplest interpretation is that H^+ must bind a single titratable group on, or closely associated with the K^+ channel and deep within the membrane electric field. Thus plausible explanations for H^+ sensitivity include cation (H^+) permeation to the binding site contributing directly to the gating as well as H^+ binding at a regulatory site on the channel protein(s), or binding altering charged/dipole components of the gating mechanism or their environment (cf. Armstrong and Lopez-Barneo, 1987; Neyton and Pelleschi, 1991). The former explanation is essentially a "gating particle" hypothesis (cf. Frankenhaeuser and Hodgkin, 1957) in which the charge displacement of H^+ to the binding site confers voltage sensitivity to the gating process. The difficulty with such a proposal is that the relatively shallow voltage dependence to H^+ binding compared with that of gating which exhibited an *e*-fold rise in current per (−)18-mV shift in voltage ($\delta \sim 1.4$; see Tables III and IV and Figs. 6 and 10). In other words, displacement of one H^+ and a single H^+-binding site alone is insufficient to account for the voltage dependence of the K^+ current.

It is worth noting, too, the striking contrast which the guard cell inward rectifier poses to known effects of H^+ on several ion channels, including K^+ channels, in animal cells (see Hille, 1984; Moody, 1984; also Hagiwara et al., 1978; Moody and Hagiwara, 1982; Cook et al., 1984; Christensen and Zeuthen, 1987; but see Tyerman et al., 1986*a*, *b*). The Na^+ channel is a good example. Protons bind with a pK_a of 5.4 (K_d = 4 μM) to a site on this channel near the external surface of the membrane (cf. Woodhull, 1973; Begenisich and Danko, 1983), but the consequence is to block and *reduce* the maximum (voltage-saturated) conductance. The observation is consistent with the general view that ions permeate channels interacting with oppositely charged groups on the surface of the channel mouth and pore (for K^+ channels, cf. MacKinnon and Miller, 1989). In this case, the H^+ sensitivity can be understood in the context of negative charge screening or voltage-dependent block by H^+ competing with Na^+ for binding within the channel pore. For the guard cell K^+ channel, however, H^+ binding *promotes* K^+ ion permeation, which must raise questions about the location of the binding site in relation to the pathway for K^+ permeation.

K^+ Inward Rectifier or Anomaly?

Two additional and distinguishing features of the guard cell inward rectifier relate to the extracellular K^+ environment; these are (*1*) a requirement for millimolar K_o^+ concentrations to activate the current, and (*2*) a voltage dependence to channel gating which is kinetically removed from this K_o^+ requirement for activity. The effect

of the K^+ concentration outside the cell goes beyond a role for the cation simply in charge movement. For the situation with 0.1 mM K_o^+ ($E_{K^+} \sim -200$ mV), current activation at voltages negative of -120 mV would imply a significant outward-directed current at intermediate potentials from -120 to -200 mV. Thus, an added role for K^+ in controlling channel gating can be inferred from the lack of any current with these voltage characteristics, even after evoking the K^+ inward rectifier (see Fig. 2 and text). The macroscopic current kinetics (Table III) offers few clues to the interaction between channel and cation in this instance, except that the activity must be fundamentally distinct from the effect(s) of voltage, and hence, of $[H^+]_o$, on channel gating kinetics. It is worth noting that a similar cation requirement has been documented for the tunicate egg inward rectifier (Ohmori, 1978).

Indeed, it is the extraordinary *in*sensitivity to K_o^+ in its voltage dependence which distinguishes the guard cell inward rectifier from the classic inward rectifiers of neuromuscular membranes and egg cells (cf. Hagiwara et al., 1976; Hagiwara and Yoshi, 1979). Gating of the latter shifts with the external K^+ concentration, so that the steady-state conductance is a function of the voltage difference $V - E_{K^+}$; by contrast, gating of the guard cell inward rectifier is independent of $[K^+]_o$ (Fig. 6 and Table III; see also Schroeder, 1988). Additionally, and unlike its animal counterparts, the guard cell K^+ current does not include an instantaneous component (compare Fig. 1 above with Fig. 2 in Hagiwara and Yoshi, 1979; Fig. 1 in Hagiwara et al., 1976).

The fixed voltage dependence of the guard cell inward rectifier also juxtaposes with that of the K^+ outward rectifier, found in the same membrane, for which the gating characteristic does follow E_{K^+} (see Blatt, 1988*a*, 1991*a*). So, it is pertinent to raise questions of channel phyllogeny and of the structural relationships between these and other K^+ channels found in eukaryotic membranes. Several of the characteristics of the guard cell inward rectifier are more commonly associated with K^+ channels which activate on (positive-going) *de*polarization. Among these features is inward rectifier sensitivity to pCa_i; like the large conductance Ca^{2+}-activated K^+ channel found in many animal cells (see Blatz and Magleby, 1987), raising $[Ca^{2+}]_i$ in the guard cells evokes a negative-going shift in the g-V characteristic for the K^+ current (Schroeder and Hagiwara, 1989; Blatt et al., 1990*b*). (Of course, the effect for the inward rectifier is to shift the activating voltages left along the voltage axis and beyond the normal physiological voltage range, by contrast with the situation for the Ca^{2+}-activated channels in the animal preparations.)

The issue is all the more provoking in light of observations that the guard cell K^+ current is blocked by nanomolar concentrations of DTX and CTX (see Fig. 5). Again, in animal preparations these toxins appear limited in action to a subfamily of outward rectifying K^+ channels (cf. Moczydlowski et al., 1988; MacKinnon and Miller, 1989; Schweitz et al., 1989). Block of the guard cell inward rectifier is consistent with high-affinity binding ($K_d \ll 50$ nM) of the toxins to the K^+ channel, and implies a significant structural homology to the several outward rectifying K^+ channels found in neuromuscular membranes. Nonetheless, any further insights must await biochemical and molecular analyses of the plant channels, and work is now underway using toxin affinity methods to purify the channel protein(s).

Physiological Implications of Channel Gating by H^+, K^+, and Voltage

The degree of H^+ sensitivity exhibited by the inward rectifier is most remarkable. The data yield a K_d about a figure of 100 nM (pK_a 7) for clamp voltages near −200 mV. So within the physiological voltage range, full activation of the current is realized in micromolar $[H^+]_o$. This situation compares favorably with inward rectifier response to intracellular free $[Ca^{2+}]$ (Schroeder and Hagiwara, 1989; Blatt et al., 1990*b*). Significantly, the pectic acids (pK_a ~3.3) that make up the bulk of acidic groups within the guard cell wall—as is generally the case within the cell walls of plants—contribute little to apoplastic buffering over the physiological range of pH_o 5–7 (cf. Saftner and Raschke, 1981; Bush and McColl, 1987; Hartung et al., 1988). Instead, the pH normally prevailing within the aqueous phase of the cell wall is subject to the net transport activity of the cells and, plausibly, also the prevailing pCO_2 (Blatt, 1987*a*; Hartung et al., 1988). In short, the H^+ dependence of the inward rectifier is so poised that pH_o is likely to play an important part in controlling K^+ flux through the channels in situ. Indeed, acid pH_o is known to promote stomatal opening (Jinno and Kuraishi, 1982), and these observations may also form a basis for understanding the early effects of atmospheric SO_2 pollution on stomata (Majernik and Mansfield, 1970; Atkinson and Winner, 1989).

There are also broader implications for stomatal function that go beyond notions of a "switch" for K^+ uptake driven by pH_o and H^+-ATPase activity (cf. Ilan et al., 1991). Gating of the K^+ inward rectifier is well suited to integrate the K^+ current with additional energetic demands on the membrane. A singular feature of plant cells is their ability to adapt to appreciable fluctuations in the extracellular ionic environment (cf. Blatt, 1991*a*). Guard cells, like other plant and fungal cells (cf. Sanders and Slayman, 1989; see also Blatt et al., 1990*a*), are able to maintain nearly constant the electrochemical driving force on H^+ ($\Delta\mu_{H^+}$) in the face of a variable pH_o (Blatt, 1987*a*; Thiel et al., 1992). This balance is achieved through the conductance of the H^+-ATPase and its pH_o dependence, and consequent variations in free-running membrane potential. Hence, voltage commonly predominates in the primary energy charge on the plant plasma membrane (Sanders and Slayman, 1989). Channel activity, in turn, must integrate within a transport economy for which the electrical, rather than the chemical gradient (ΔpH) is paramount; in short, the energetic requirements for channel activity—its voltage-dependence and current drain—must balance with the needs of other cellular homeostatic functions.

The H^+ dependence inherent to gating of the K^+ inward rectifier may be seen to anticipate and compensate for the pH_o dependence liable of the H^+-ATPase. To illustrate this point, steady-state *I-V* characteristics for the H^+-ATPase were calculated using the kinetic parameters determined from *Vicia* guard cells (Blatt, 1987*b*, 1988*c*); these curves are compared in Fig. 14 with steady-state *I-V* characteristics for the inward rectifier recorded over the same pH_o range. The principle effect expected of alkaline-going pH_o is that the *I-V* characteristic for the H^+-ATPase shifts to the left (negative-going) along the voltage axis (cf. Blatt et al., 1990*a*). Gating of the inward rectifier tracks the H^+-ATPase so that, with alkaline-going pH_o, the K^+ current activates at increasingly negative voltages. All other factors being equal, similar rates of K^+ uptake might be realized with a similar pump output at each pH_o, but at

increasingly negative free-running potentials reflecting the balance of membrane voltage in the primary H^+ electrochemical gradient at neutral and alkaline pH_o. So the predicted effect is to displace the voltage dependence for K^+ uptake with pump output, ensuring that the inward rectifier cannot short-circuit other energetic demands on membrane voltage irrespective of the prevailing extracellular H^+ concentration.

Likewise, the K_o^+-related characteristics of the K^+ inward rectifier are equally well accommodated to the requirements of an H^+-coupling membrane. One consequence of a fixed (K_o^+ constant) voltage dependence for the inward rectifier is to enforce a

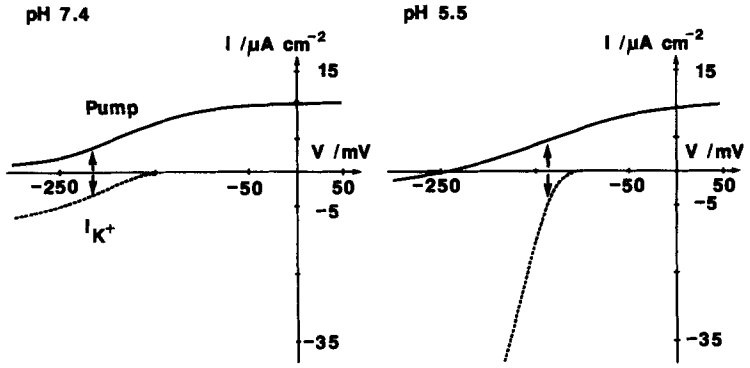

FIGURE 14. Kinetic coordination of H^+-ATPase and K^+ inward rectifier. Pump (——) and channel (····) currents at pH_o 7.4 (*left*) and 5.5 (*right*). Arrows mirrored on the voltage axis mark the voltages at which the currents are equal in magnitude. Note the roughly equivalent current magnitudes predicted when currents balance in each case, despite a ~ +90-mV shift to the acid pH. Representative K^+ currents were taken from one *Vicia* guard cell bathed in 10 mM KCl. H^+ pump currents were calculated from Class I, two-state reaction kinetic analyses carried out at pH_o 7.4 and incorporating a pH_o dependence in the reaction constant for carrier H^+ debinding/recycling (see Blatt, 1987*b*, 1988*c*; also Blatt et al., 1990*a*). The parameters and corresponding pump equilibrium potential (E_p) were,

	K_{io}^o	k_{oi}^o	K_{io}	K_{oi}	E_p
pH_o 7.4	500	0.04	0.1	10	−358
pH_o 5.5	200	0.04	3.3	10	−244

minimum polarization of the membrane for K^+ uptake (at pH_o 6.1, to voltages greater than (−)120–140 mV [see Figs. 5–8]) irrespective of E_{K^+} and the prevailing K_o^+ concentration. As a result, the K^+ conductance cannot overwhelm the membrane between E_{K^+} and this "gating voltage." Taking 10 mM K_o^+ as an example, voltages in excess of (−)150 mV may be achieved (Thiel et al., 1992) with relatively little expenditure of energy by the pump, despite the large driving force for K^+ influx across the plasma membrane (-80 mV $< E_{K^+} < -60$ mV typical). Again, gating of the inward rectifier may be seen to ensure that K^+ uptake cannot short-circuit other energetic demands on membrane voltage.

The requirement for millimolar K_o^+ to evoke the current also complements this control strategy. Such a fixed voltage dependence is effective so long as the extracellular K^+ environment remains within fixed limits; for guard cells to effect net K^+ uptake via the inward rectifier, the current must activate at voltages negative to E_{K^+}. Practically speaking, these needs are met for $[K^+]_o > 1$ mM (see also Thiel et al., 1992); but in submillimolar K_o^+, the inward rectifier could present a pathway for net K^+ efflux over a wide voltage range (from −120 to −200 mV in 0.1 mM K_o^+; see above; also Blatt, 1991*a*). In fact, the circumstance does not arise because of the K_o^+ requirement for channel activity. Instead, energy-coupled mechanisms for K^+ uptake are likely to be important in submillimolar K_o^+ (see Clint and Blatt, 1989).

pH and the K^+ Outward Rectifier

Current passage through the K^+ outward rectifier also responds to $[H^+]$, although the action appears to reflect a sensitivity to pH on the cytoplasmic side of the membrane (see Fig. 13). Superficially, block by acid pH parallels similar observations in a variety of animal cells (see Cook et al., 1984; Moody, 1984; Christensen and Zeuthen, 1987) and in the giant alga *Nitella* (Sokolik and Yurin, 1986) but again there are some important differences in this case; notably, the effect of pH on the guard cell K^+ current appears largely independent of membrane voltage (see Figs. 9 and 13).

These data raise one final issue related to the physiological controls on this current. Parallel flux and electrical measurements have yielded strong evidence that the outward rectifier is the dominant pathway for K^+ efflux from guard cells (Clint and Blatt, 1989). The phytohormone abscisic acid (ABA), which acts as a water stress signal in higher plants and potentiates stomatal closing, activates this current in a voltage-independent manner, either by recruiting channels or affecting single channel conductance (Blatt, 1990; Thiel et al., 1992). ABA action extends also to the K^+ inward rectifier and to one or more Cl^- (anion) channels in the guard cell plasma membrane (cf. Blatt, 1990; Hedrich et al., 1990; Thiel et al., 1992), and much attention has been drawn to the coupling between these currents and the phytohormone, mediated by cytoplasmic free Ca^{2+} and inositol trisphosphate-dependent Ca^{2+} release (Schroeder and Hagiwara, 1989; Blatt et al., 1990*b*; Gilroy et al., 1990; McAinsh et al., 1990; also the review by Blatt, 1991*a*). Significantly, gating of the K^+ outward rectifier is singularly *in*sensitive to Ca^{2+} concentration on the cytoplasmic face of the membrane (Hosoi et al., 1988; Schroeder and Hagiwara, 1989; Blatt et al., 1990*b*); the implication is that additional but as yet unidentified signaling pathways must function in parallel with those that appear to control the K^+ inward rectifier and the other inward-going currents (see Blatt, 1991*a* for review).

Considerable evidence, albeit circumstantial, can be marshaled now which implicates cytoplasmic $[H^+]$ as this "missing" signal intermediate. Most important, there are strong indications that the $[H^+]_i$ dependence of the K^+ outward rectifier extends over the physiological pH_i range. Not only is this current selectively reduced or eliminated by intracellular acid loads (Fig. 13), it also appears to be enhanced by alkaline pH_i: an overshoot in the K^+ current has been observed to follow channel block with TEA and was ascribed to cytoplasmic alkalinization and its recovery (Blatt and Clint, 1989) imposed by an impurity in TEA, triethylamine. Furthermore, the effects of pH_i and ABA are kinetically similar, in all cases the current responding in a

largely voltage-independent manner (see also Blatt and Clint, 1989; Blatt, 1990). Finally, ABA has been reported to induce cytoplasmic alkalinizations together with a rise in free Ca^{2+} concentration in *Zea* coleoptile tissues (Gehring et al., 1990). Key questions now under investigation are whether the K^+ outward rectifier response can be linked to a similar course of events in the guard cells and, equally important, whether the origin of any ABA-evoked pH_i signal can be ascertained.

I am grateful to E. A. C. MacRobbie (Botany School, University of Cambridge) and D. A. Baker (University London, Wye College) for their support, and to G. Thiel (University of Göttingen), S. Hladky (Department of Pharmacology, University of Cambridge), and P. McNaughton (University of London, Kings' College) for many helpful discussions and comments on the manuscript.

This work was aided by an equipment grant from the Gatsby Charitable Trust.

Original version received 6 May 1991 and accepted version received 19 December 1991.

REFERENCES

Armstrong, C. M., and J. Lopez-Barneo. 1987. External calcium ions are required for potassium channel gating in squid neurons. *Science.* 236:712–714.

Atkinson, C. J., and W. E. Winner. 1989. Modification of stomatal conductance by sulphur dioxide. *Journal of Experimental Botany.* 40:461–467.

Baier, M., and W. Hartung. 1988. Movement of abscisic acid across the plasmalemma and the tonoplast of guard cells of *Valerianella locusta. Botanica Acta.* 101:332–337.

Begenisich, T. B., and M. Danko. 1983. Hydrogen ion block of the sodium pore in squid giant axons. *Journal of General Physiology.* 82:599–618.

Beilby, M. J. 1990. Current-voltage curves for plant membrane studies: a critical analysis of the method. *Journal of Experimental Botany.* 41:165–182.

Blatt, M. R. 1987*a*. Electrical characteristics of stomatal guard cells: the ionic basis of the membrane potential and the consequence of potassium chloride leakage from microelectrodes. *Planta.* 170:272–287.

Blatt, M. R. 1987*b*. Electrical characteristics of stomatal guard cells: the contribution of ATP-dependent, "electrogenic" transport revealed by current-voltage and difference-current-voltage analysis. *Journal of Membrane Biology.* 98:257–274.

Blatt, M. R. 1988*a*. Potassium-dependent bipolar gating of potassium channels in guard cells. *Journal of Membrane Biology.* 102:235–246.

Blatt, M. R. 1988*b*. Potassium channel gating in guard cells depends on external K^+ concentration. *Plant Physiology.* 86:826A. (Abstr.)

Blatt, M. R. 1988*c*. Mechanisms of fusicoccin action: a dominant role for secondary transport in a higher-plant cell. *Planta.* 174:187–200.

Blatt, M. R. 1990. Potassium channel currents in intact stomatal guard cells: rapid enhancement by abscisic acid. *Planta.* 180:445–455.

Blatt, M. R. 1991*a*. Ion channel gating in plants: physiological implications and integration for stomatal function. *Journal of Membrane Biology.* 124:95–112.

Blatt, M. R. 1991*b*. A primer in plant electrophysiological methods. *In* Methods in Plant Biochemistry. K. Hostettmann, editor. Academic Press, London. 281–321.

Blatt, M. R., M. J. Beilby, and M. Tester. 1990*a*. Voltage dependence of the *Chara* proton pump revealed by current-voltage measurement during rapid metabolic blockade with cyanide. *Journal of Membrane Biology.* 114:205–223.

Blatt, M. R., and G. M. Clint. 1989. Mechanisms of fusicoccin action kinetic modification and inactivation of potassium channels in guard cells. *Planta*. 178:509–523.

Blatt, M. R., G. Thiel, and D. R. Trentham. 1990*b*. Reversible inactivation of K^+ channels of *Vicia* stomatal guard cells following the photolysis of caged inositol 1,4,5-trisphosphate. *Nature*. 346: 766–769.

Blatz, A. L., and K. L. Magleby. 1987. Calcium-activated potassium channels. *Trends in Neuroscience*. 10:463–467.

Busch, H., R. Hedrich, and K. Raschke. 1990. External calcium block inward rectifier potassium channels in guard cell protoplasts in a voltage and concentration dependent manner. *Plant Physiology*. 93:96A. (Abstr.)

Bush, D. S., and J. G. McColl. 1987. Mass-action expressions of ion exchange applied to Ca^{2+}, H^+, K^+ and Mg^{2+} sorption on isolated cell walls of leaves from *Brassica oleracea*. *Plant Physiology*. 85:247–260.

Christensen, O., and T. Zeuthen. 1987. Maxi K^+ channels in leaky epithelia are regulated by intracellular Ca^{2+}, pH and membrane potential. *Pflügers Archiv*. 408:249–259.

Clint, G. M., and M. R. Blatt. 1989. Mechanisms of fusicoccin action: evidence for concerted modulations of secondary K^+ transport in a higher-plant cell. *Planta*. 178:495–508.

Cook, D. L., M. Ikeuchi, and W. Y. Fujimoto. 1984. Lowering of pH_i inhibits Ca^{2+}-activated K^+ channels in pancreatic B-cells. *Nature*. 311:269–271.

Eisenman, G., and R. Horn. 1983. Ion selectivity revisited: the role of kinetic and equilibrium processes in ion permeation through channels. *Journal of Membrane Biology*. 76:197–225.

Felle, H. 1988*a*. Cytoplasmic free calcium in *Riccia fluitans* L. and *Zea mays* L.: interaction of Ca^{2+} and pH? *Planta*. 176:248–255.

Felle, H. 1988*b*. Auxin causes oscillations of cytosolic free calcium and pH in *Zea mays* coleoptiles. *Planta*. 174:495–499.

Frankenhaeuser, B., and A. L. Hodgkin. 1957. The action of calcium on the electrical properties of squid axons. *Journal of Physiology*. 137:218–244.

Gehring, C. A., H. R. Irving, and R. W. Parish. 1990. Effects of auxin and abscisic acid on cytosolic calcium and pH in plant cells. *Proceedings of the National Academy of Sciences, USA*. 87:9645–9649.

Gilroy, S., N. D. Read, and A. J. Trewavas. 1990. Elevation of cytoplasmic calcium by caged calcium or caged inositol trisphosphate initiates stomatal closure. *Nature*. 346:769–771.

Hagiwara, S., S. Miyazaki, and N. P. Rosenthal. 1976. Potassium current and the effect of cesium on this current during anomalous rectification of the egg cell membrane of a starfish. *Journal of General Physiology*. 67:621–638.

Hagiwara, S., S. Myazaki, W. Moody, and J. Patlak. 1978. Blocking effects of barium and hydrogen ions on the potassium current during anomalous rectification in the starfish egg. *Journal of Physiology*. 279:167–185.

Hagiwara, S., and M. Yoshii. 1979. Effects of internal potassium and sodium on the anomalous rectification of the starfish egg as examined by internal perfusion. *Journal of Physiology*. 292:251–265.

Hartung, W., J. W. Radin, and D. L. Hendrix. 1988. Abscisic acid movement into the apoplastic solution of water-stressed cotton leaves. *Physiologica Plantarum*. 86:908–913.

Hedrich, R., H. Busch, and K. Raschke. 1990. Ca^{2+} and nucleotide dependent regulation of voltage dependent anion channels in the plasma membrane of guard cells. *European Molecular Biology Organisation Journal*. 9:3889–3892.

Hedrich, R., and J. I. Schroeder. 1989. The physiology of ion channels and electrogenic pumps in higher plants. *Annual Review of Plant Physiology and Molecular Biology*. 40:539–569.

Hille, B. 1973. Potassium channels in myelinated nerve. *Journal of General Physiology*. 61:669–686.

Hille, B. 1984. Ion Channels of Excitable Membranes. Sinauer Associates, Inc., Sunderland, MA.

Hille, B., A. M. Woodhull, and B. I. Shapiro. 1975. Negative surface charge near sodium channels of nerve: divalent ions, monovalent ions and pH. *Philosophical Transactions of the Royal Society of London, B.* 270:301–318.

Hodgkin, A. L., A. F. Huxley, and B. Katz. 1952. Measurements of current-voltage relations in the membrane of the giant axon of *Loligo*. *Journal of Physiology.* 116:424–448.

Hosoi, S., M. Iino, and K. Shimazaki. 1988. Outward-rectifying K^+ channels in stomatal guard cell protoplasts. *Plant and Cell Physiology.* 29:907–911.

Ilan, N., A. Schwartz, and N. Moran. 1991. pH effect on K^+ channels in plasmalemma of guard cell protoplasts. *Plant Physiology.* 96:912A. (Abstr.)

Jinno, N., and S. Kuraishi. 1982. Acid-induced stomatal opening in *Commelina communis* and *Vicia faba*. *Plant and Cell Physiology.* 23:1169–1174.

Kurkdjian, A., and J. Guern. 1989. Intracellular pH: measurement and importance in cell activity. *Annual Review of Plant Physiology and Molecular Biology.* 40:271–303.

Majernik, O., and T. A. Mansfield. 1970. Direct effects of SO_2 pollution on the degree of stomatal opening. *Nature.* 277:377–378.

MacKinnon, R., and C. Miller. 1989. Mutant potassium channels with altered binding of charybdotoxin, a pore-blocking peptide inhibitor. *Science.* 245:1382–1385.

Marquardt, D. 1963. An algorithm for least-squares estimation of nonlinear parameters. *Journal of the Society of Industrial and Applied Mathematics.* 11:431–441.

McAinsh, M. R., C. Brownlee, and A. M. Hetherington. 1990. Abscisic acid-induced elevation of guard cell cytosolic Ca^{2+} precedes stomatal closure. *Nature.* 343:186–188.

Moczydlowski, E., K. Lucchesi, and A. Ravindran. 1988. An emerging pharmacology of peptide toxins targeted against potassium channels. *Journal of Membrane Biology.* 105:95–111.

Moody, W., Jr. 1984. Effects of intracellular H^+ on the electrical properties of excitable cells. *Annual Review of Neuroscience.* 7:257–278.

Moody, W. J., and S. Hagiwara. 1982. Block of inward rectification by intracellular H^+ in immature oocytes of the starfish *Mediaster aequalis*. *Journal of General Physiology.* 79:115–130.

Neyton, J., and M. Pelleschi. 1991. Multi-ion occupancy alters gating in high-conductance, Ca^{2+}-activated K^+ channels. *Journal of General Physiology.* 97:641–665.

Ohmori, H. 1978. Inactivation kinetics and steady-state current noise in the anomalous rectifier of tunicate egg cell membranes. *Journal of Physiology.* 281:77–99.

Rodriguez-Navarro, A., M. R. Blatt, and C. L. Slayman. 1986. A potassium-proton symport in *Neurospora crassa*. *Journal of General Physiology.* 87:649–674.

Saftner, R. A., and K. Raschke. 1981. Electrical potentials in stomatal complexes. *Plant Physiology.* 67:1124–1132.

Sanders, D., and C. L. Slayman. 1982. Control of intracellular pH: predominant role of oxidative metabolism, not proton transport, in the eukaryotic microorganism *Neurospora*. *Journal of General Physiology.* 80:377–402.

Sanders, D., and C. L. Slayman. 1989. Transport at the plasma membrane of plant cells: a review. *In* Plant Membrane Transport: The Current Position. J. Dainty, M. I. De Michelis, E. Marre, and F. Rasi-Caldogno, editors. Elsevier Science Publishers B. V., Amsterdam. 3–11.

Schroeder, J. I. 1988. K^+ transport properties of K^+ channels in the plasma membrane of *Vicia faba* guard cells. *Journal of General Physiology.* 92:667–683.

Schroeder, J. I., and S. Hagiwara. 1989. Cytosolic calcium regulates ion channels in the plasma membrane of *Vicia faba* guard cells. *Nature.* 338:427–430.

Schroeder, J. I., K. Raschke, and E. Neher. 1987. Voltage dependence of K^+ channels in guard-cell protoplasts. *Proceedings of the National Academy of Sciences, USA.* 84:4108–4112.

Schweitz, H., C. E. Stansfeld, J.-N. Bidard, L. Fagni, P. Maes, and M. Lazdunski. 1989. Charybdotoxin blocks dendrotoxin-sensitive voltage-activated K^+ channels. *FEBS Letters.* 250:519–522.

Sokolik, A. I., and V. M. Yurin. 1986. Potassium channels in plasmalemma of *Nitella* cells at rest. *Journal of Membrane Biology.* 89:9–22.

Standen, N. B., and P. R. Stanfield. 1979. Potassium depletion and sodium block of potassium currents under hyperpolarization in frog sartorius muscle. *Journal of Physiology.* 294:497–520.

Tester, M. 1988. Pharmacology of potassium channels in the plasmalemma of the green alga chara-corallina. *Journal of Membrane Biology.* 103:159–170.

Thiel, G., E. A. C. MacRobbie, and M. R. Blatt. 1992. Current-voltage characteristics of two states of the guard cell plasma membrane and their implications for voltage control of ion transport. *Journal of Membrane Biology.* In press.

Tyerman, S. D., G. P. Findlay, and G. J. Paterson. 1986*a*. Inward membrane current in *Chara inflata:* I. A voltage- and time-dependent Cl^- component. *Journal of Membrane Biology.* 89:139–152.

Tyerman, S. D., G. P. Findlay, and G. J. Paterson. 1986*b*. Inward membrane current in *Chara inflata:* II. Effects of pH, Cl^--channel blockers and NH_4^+, and significance for the hyperpolarised state. *Journal of Membrane Biology.* 89:153–161.

Waddell, W. J., and R. G. Bates. 1969. Intracellular pH. *Physiological Reviews.* 49:185–329.

Wagner, R., E. C. Apley, and W. Hanke. 1989. Single channel H^+ currents through reconstituted chloroplast ATP synthase CF_0-CF_1. *EMBO Journal.* 8:2827–2834.

Woodhull, A. M. 1973. Ionic blockage of sodium channels in nerve. *Journal of General Physiology.* 61:687–708.